



**HAL**  
open science

## Nano-mechanical properties of starch and gluten biopolymers from atomic force microscopy

Emna Chichti, Matthieu George, Jean-Yves Delenne, Farhang Radjai, Valérie Lullien-Pellerin

► **To cite this version:**

Emna Chichti, Matthieu George, Jean-Yves Delenne, Farhang Radjai, Valérie Lullien-Pellerin. Nano-mechanical properties of starch and gluten biopolymers from atomic force microscopy. *European Polymer Journal*, 2013, 49 (12), pp.3788-3795. 10.1016/j.eurpolymj.2013.08.024 . hal-02648905

**HAL Id: hal-02648905**

**<https://hal.inrae.fr/hal-02648905>**

Submitted on 30 Jul 2024

**HAL** is a multi-disciplinary open access archive for the deposit and dissemination of scientific research documents, whether they are published or not. The documents may come from teaching and research institutions in France or abroad, or from public or private research centers.

L'archive ouverte pluridisciplinaire **HAL**, est destinée au dépôt et à la diffusion de documents scientifiques de niveau recherche, publiés ou non, émanant des établissements d'enseignement et de recherche français ou étrangers, des laboratoires publics ou privés.

Manuscript Number: EUROPOL-D-13-00611R1

Title: Nano-mechanical properties of starch and gluten biopolymers from Atomic Force Microscopy

Article Type: Research Paper

Section/Category: Nanotechnology

Keywords: AFM; Biopolymer; Hardness; Friction; Scratch test

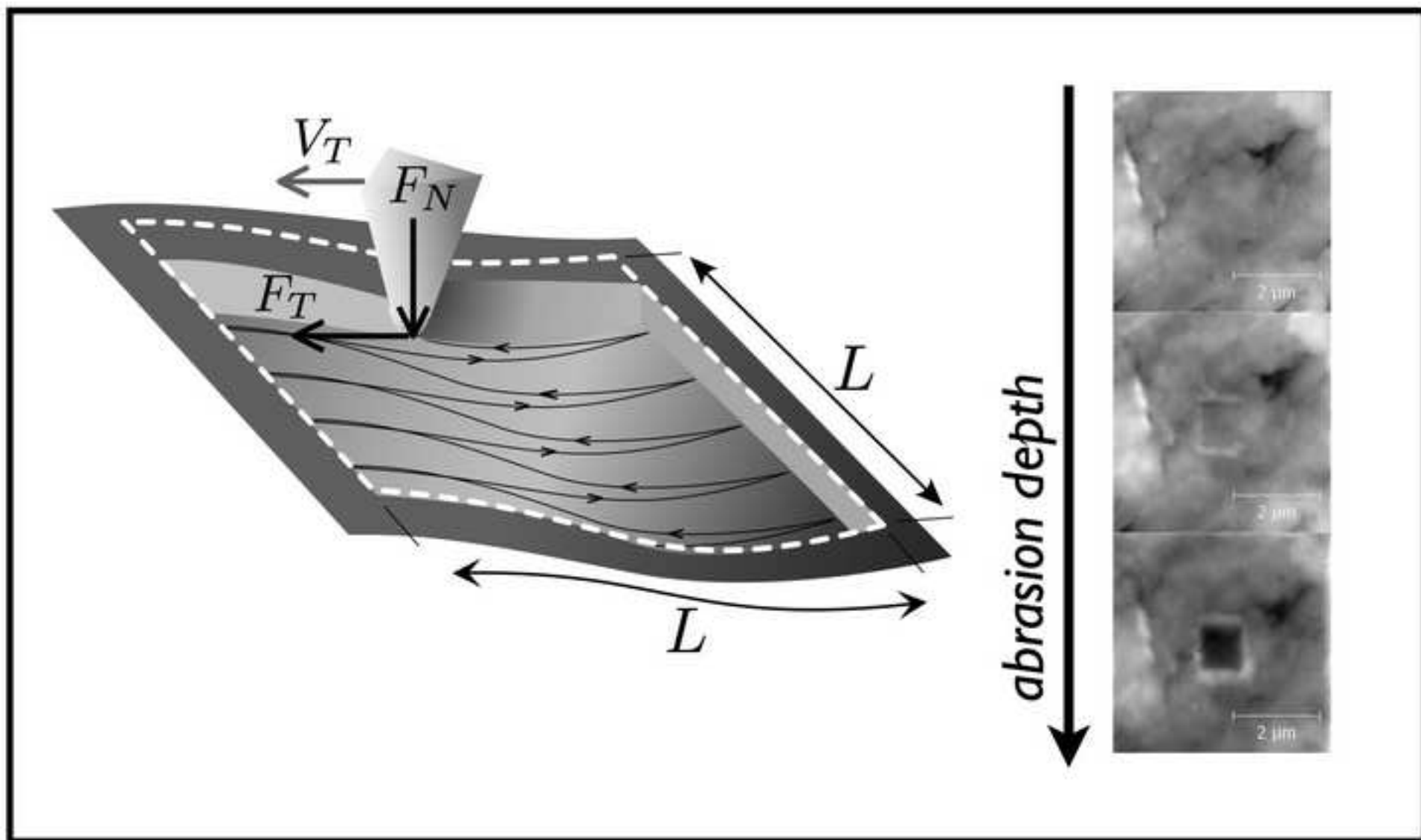
Corresponding Author: Dr. Valérie Lullien-Pellerin,

Corresponding Author's Institution:

First Author: Emna Chichti

Order of Authors: Emna Chichti; Mathieu George; Jean-Yves Delenne; Fahrang Radjai; Valérie Lullien-Pellerin

Abstract: An original method based on atomic force microscopy (AFM) in contact mode was developed to abrade progressively the surface of tablets made of starch or gluten polymers isolated from wheat. The volume of the material removed by the tip was estimated from the analysis of successive topographic images of the surface, and the shear force was measured by keeping a constant normal force. Our data together with a simple tribological model provide clear evidence for a higher hardness and shear strength of starch compared to gluten. Gluten appears to have mechanical properties close to soft materials, such as talc, whereas starch displays higher hardness close to calcite. Our results are in a better agreement with structural properties of gluten (complex protein network) and starch (granular and semi-cristalline structure) than earlier studies by micro-indentation. This work shows that the AFM scratching method is relevant for the characterization of any polymer surface, in particular in application to materials made of different polymers at the nano-scale.



## Highlights

- Scratching with AFM tip was used to screen polymer resistance
- A tribological model was developed to determine polymer hardness
- The methodology is used to reveal hardness contrasts in biomaterials at nanoscale
- Wheat starch was found to display higher hardness and shear strength than gluten

# Nano-mechanical properties of starch and gluten biopolymers from Atomic Force Microscopy

Emna Chichti<sup>a,c</sup>, Matthieu George<sup>b</sup>, Jean-Yves Delenne<sup>a</sup>, Farhang Radjai<sup>c</sup>,  
Valérie Lullien-Pellerin<sup>a,1</sup>

<sup>a</sup>*INRA, UMR 1208, Ingénierie des Agropolymères et Technologies Emergentes, F-34060  
Montpellier Cedex 01, France*

<sup>b</sup>*Laboratoire Charles Coulomb, UMR 5221, CNRS-UM2, Place Eugène Bataillon,  
F-34095 Montpellier Cedex, France*

<sup>c</sup>*Laboratoire de Mécanique et Génie Civil, UMR 5508, CNRS-UM2, Place Eugène  
Bataillon, F-34095 Montpellier, France*

---

## Abstract

An original method based on atomic force microscopy (AFM) in contact mode was developed to abrade progressively the surface of tablets made of starch or gluten polymers isolated from wheat. The volume of the material removed by the tip was estimated from the analysis of successive topographic images of the surface, and the shear force was measured by keeping a constant normal force. Our data together with a simple tribological model provide clear evidence for a higher hardness and shear strength of starch compared to gluten. Gluten appears to have mechanical properties close to soft materials, such as talc, whereas starch displays higher hardness close to calcite. Our results are in a better agreement with structural properties of gluten (complex protein network) and starch (granular and semi-cristalline structure) than earlier studies by micro-indentation. This work shows that the AFM scratching method is relevant for the characterization of any polymer surface, in particular in application to materials made of different polymers at the nano-scale.

*Keywords:* AFM, Biopolymer, Hardness, Friction, Scratch test

---

<sup>1</sup>Corresponding author. Tel: +33 4 99 61 31 05  
Email address: lullien@supagro.inra.fr (V. Lullien-Pellerin)

## 1. Introduction

Wheat is a major cereal crop for both food and non-food industries. The starchy endosperm, which is the main constituent of wheat grains (80-85%), contains two important biopolymers, which display unique rheological properties [1, 2, 3] : starch (80-90% of dry mass) in the form of granules which are embedded in a gluten matrix, mainly made of the storage proteins [4].

Food products, such as bread, biscuits or pasta, are made of flour and semolina which are obtained by the isolation of wheat grain endosperm and its reduction by dry fractionation in successive steps of grinding and sieving. In turn, further processing of flour and semolina can be undertaken to isolate starch and gluten biopolymers which are used in food industry, e.g. as additives to adjust food rheology, and in non-food applications to replace petroleum-based packaging materials [5, 6, 7], coating agents in paper industries [8, 9] or adhesives [10, 11] due to their renewability, physical properties and biodegradability. Purified starch is also employed as a starting material in petrochemical processes [9].

Therefore for a better control of the endosperm product quality, it is necessary to better characterize the fractionation behavior of the wheat endosperm which is clearly related to its structure and mechanical properties. The endosperm structure could be related to a granular cemented material and a numerical model was built in order to identify key factors, which could play a role in its mechanical behaviour [12, 13]. The model was based on actual knowledge of the endosperm structure and organization and took into account the described mechanical properties of starch and protein that were reported to be identical based on micro-indentation assays [14, 15]. The model showed that the fracture propagates differently depending on both the protein content and the starch/protein matrix adhesion. However, lack of information about the polymer mechanical properties at a nano-scale constitutes a major limitation for the modeling construction.

In this paper, we investigate the mechanical properties of isolated unmodified wheat starch and gluten with an original AFM nanoscratch approach. Since its invention [16], AFM has proved to be a powerful tool for topographical imaging at the nanoscale and with minimal sample preparation, of various biomolecules such as nucleic acids, proteins, polysaccharides, but also for the measurement of their mechanical properties [17, 18]. AFM has already been employed to characterize the surface topography of wheat starch and to compare its structure to starch isolated from other plant resources

38 [19, 20]. Similar topographic studies were also reported for some of the  
39 storage proteins forming the gluten network. Gliadins ( $\alpha, \omega$ ) interactions in  
40 different solvent conditions [21], as well as non-covalent interactions between  
41 glutenins of high molecular weight [22], have been investigated by means of  
42 AFM but with slight modifications of the molecules by either immobilisa-  
43 tion or reduction and alkylation. Wheat endosperm was also tentatively  
44 observed using AFM to compare the endosperm structure in wheat grains  
45 differing by their hardness, but the method was unable to discern between  
46 starch and gluten polymers even if some differences in surface morphology  
47 were observed depending on the wheat genetic origin [23].

48 Indentation or scratching assays are generally used to probe the mechan-  
49 ical properties of different polymers from the nano to micro-scale [24, 25].  
50 Recently, Kurland et al. [26] reviewed how AFM could be used for nano-  
51 indentation under native conditions to access the Young modulus of globular,  
52 fibrous and filamentous proteins. New developments have also been reported  
53 on the use of an AFM tip to abrade a target sample surface for the measure-  
54 ment of cohesive energy in a biological material [27]. Similar scratching tests  
55 on polymers by means of a nanoindenter were used for friction analysis [28]  
56 and determination of shear strength [29]. But, to our best knowledge, AFM  
57 has never been used as a tool to characterize the mechanical properties, i.e.  
58 hardness and shear stress of such biopolymers as starch and gluten. In the  
59 following, we first present our materials and AFM nanoscratch method. The  
60 data will then be analyzed for starch and gluten samples and used to deter-  
61 mine their hardness and apparent friction coefficients. A simple tribological  
62 model will be used to approach the shear strength of both polymers. Finally,  
63 we conclude with the most salient findings and perspectives of this work.

## 64 **2. Experimental**

### 65 *2.1. Materials*

66 All commercial products, wheat starch (Fluka N°85649,  $\leq 0.5\%$  ash,  
67  $10.5\%$  water content) and gluten biopolymer (SigmaG5004,  $80\%$  protein,  $7\%$   
68 fat,  $7.5\%$  water content) were purchased from Sigma-Aldrich Co (St-Louis,  
69 MO, USA). Starch ( $98\%$  purity,  $11.5\%$  moisture content) and gluten ( $65\%$   
70 purity,  $9.5\%$  moisture content) were also purified from wheat grains display-  
71 ing distinct hardnesses (hard and soft common wheat cv. Glasgow and Di-  
72 nosor, respectively) using a previously described method [30]. Polymethyl  
73 methacrylate (PMMA, Fluka 183350,  $T_g = 124^\circ C$ , of average molecular

74 weight  $1.2 \cdot 10^6$  g/mol), was used as reference material with known mechan-  
75 ical properties at the nanoscale [31, 25, 32].

## 76 2.2. Sample preparation

77 Several tablets of commercial or extracted starch and gluten powders were  
78 prepared with approximate weight of 1 g in a pelletizer (Specac Inc, Smyrna,  
79 USA) by applying a pressure of 0.5 MPa during one minute using a laboratory  
80 press (Hydraulische Press, Perkin-Elmer, USA). Tablets were stored before  
81 analysis under controlled conditions of temperature and humidity ( $20^\circ\text{C}$ , 30%  
82 RH).

## 83 2.3. Microscopy

84 Environmental Scanning Electron Microscopy (ESEM, Fei Quanta 200  
85 FEG, FEI Co, Hillsboro, OR, USA) without sputter coating was used to  
86 check the homogeneity and absence of defaults in the samples as well as for  
87 imaging AFM tips before and after abrasion.

## 88 2.4. AFM assays

89 AFM assays were performed with a Nanoscope V atomic force microscope  
90 (Bruker instruments, Madison, WI, USA), operating in the contact mode  
91 under controlled conditions of temperature and humidity ( $20^\circ\text{C}$ , 30% rela-  
92 tive humidity). Commercial  $\text{Si}_3\text{N}_4$  tips (Bruker) mounted on a rectangular  
93 cantilever with stiffness in the range between 1 and 5 N/m were chosen to  
94 preserve reasonable measurement sensitivity and to exert sufficiently large  
95 forces to abrade the samples. Before each measurement, the normal and tan-  
96 gential forces  $F_N$  and  $F_T$ , respectively, were calibrated by means of a hard  
97 silicon wafer in order to convert the values measured in volts to force units.

98 The calibration of the normal force was performed through displacement-  
99 force plots whereas vertical cantilever stiffness measurements were calibrated  
100 by means of the thermal fluctuation method [33]. The friction forces were  
101 calibrated using Coulomb's friction law and the value of the friction coeffi-  
102 cient for the silicon wafer was fixed ( $\mu_{\text{Si-Si}} = 0.1$ ) according to the studies of  
103 Morton et al. [34]. Since AFM calibration was made on hard silicon wafers,  
104 the tips are expected to be partially flattened. Several ESEM observations  
105 were made, as illustrated in Figure 1a, in order to check the tip geometry  
106 before and after calibration. The contacting areas of the tips were character-  
107 ized through reverse imaging obtained with AFM (Figure 1b) on a calibrating



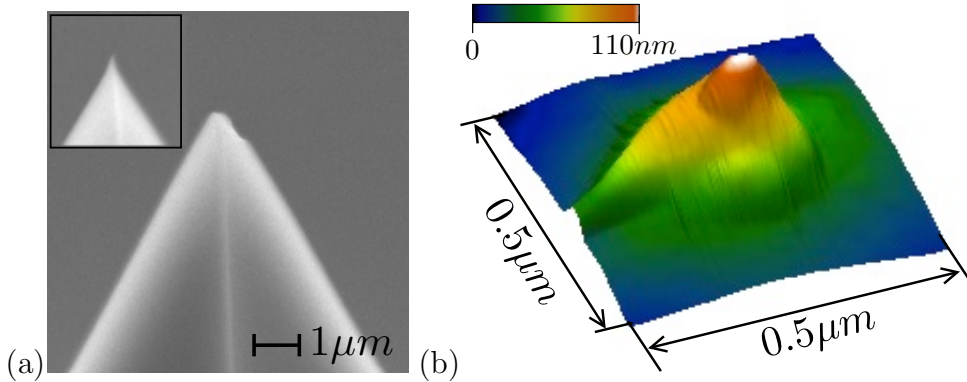


Figure 1: a) ESEM pictures of an AFM tip before (insert) and after calibration; b) Picture in false colors of an AFM tip obtained by mirror imaging with a calibrating grid.

108 grid of equally-spaced sharp points of apex radius  $\simeq 10$  nm (TGT01, Mikro-  
 109 masch, Inc., Estonia). These measurements clearly showed that the AFM  
 110 tip apex can be well fitted after calibration by a sphere from the extremity  
 111 to 20 nm high, with an average radius for the set of tips  $R = 82 \pm 32$  nm.

112 The AFM assays were conducted, as schematized in Figure 2a, by follow-  
 113 ing a procedure inspired by a previously described method [27]. It consists of  
 114 successive steps of topographic image acquisition on a large scale and abra-  
 115 sive scans on a predefined area by setting the force applied on the AFM  
 116 cantilever to the desired value. First, a large ( $L \times L > 10 \times 10 \mu\text{m}^2$ ) topo-  
 117 graphic image is acquired as the tip scans the sample surface at a low applied  
 118 normal force ( $F_N = 100\text{nN}$ ) in order to select the appropriate working area  
 119 for polymer abrasion, i.e. the center of a starch granule or a homogeneous  
 120 gluten area. Then, a smaller topographic image ( $5 \times 5\mu\text{m}^2$ ) at a scan tip  
 121 velocity  $V_T$  of  $10 \mu\text{m/s}$  ( $512 \times 512$  pixels) is acquired (step 1) inside the se-  
 122 lected area in identical conditions, that will serve as reference image of the  
 123 undamaged surface.

124 The abrasion process (step 2) is initiated on the central area ( $L \times L = 1 \times 1$   
 125  $\mu\text{m}^2$ ) with an increase of the applied normal force ( $F_N > 200$  nN) and a de-  
 126 crease of the scan velocity ( $V_T = 2 \mu\text{m/s}$ ,  $256 \times 256$  pixels). Both the trace  
 127 and retrace  $F_T$  force maps are acquired (respectively scanning from left side  
 128 to right side of the image and from right side to left side) to determine  
 129 the average force sustained by the sample in the direction of displacement.  
 130 Thereafter, the normal force is decreased back (step 3) to its initial value (100  
 131 nN) and a second topographic image ( $5 \times 5 \mu\text{m}^2$ ) is recorded at  $V_T = 10$

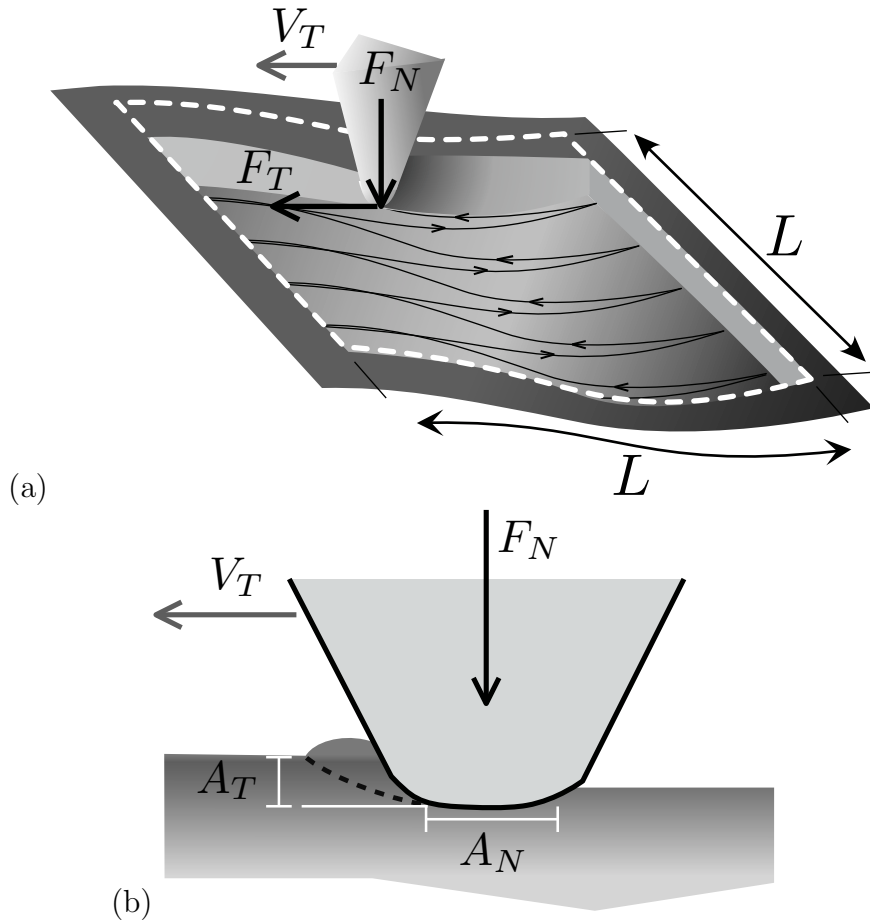


Figure 2: a) Schematic representation of the AFM procedure where  $F_N$  is the applied normal force,  $V_T$  is scan tip velocity,  $F_T$  is friction force and  $L$  is the length of the abraded area; b) Schematic description of the abrasion zone where  $A_N$  is the projected contact area of the tip on the sample surface and  $A_T$  is the projected area in front of the tip in the direction of displacement.

132  $\mu\text{m/s}$  before increasing again the normal force to further abrade the material.  
133 A progressive and controlled abrasion of the polymer sample was ensured by  
134 repeating up to ten times the abrasion step (step 2), interrupted by regular  
135 acquisitions of larger topographic images (step 1) after  $N = 1, 4, 7$  and 10  
136 abrasive scans, respectively. This abrasion process was undertaken at least  
137 on ten distinct independent locations for each analysed polymer. The ac-  
138 quired AFM images were visualized and analyzed by means of the software  
139 Gwyddion 2.26 (Department of Nanometrology, Czech Metrology Institute,  
140 Brno, CZ) in order to evaluate the abrasion depth and friction force  $F_T$ .

### 141 2.5. Nano-indentation assays

142 Nano-indentation assays were performed using a diamond Berkovich in-  
143 denter (CSM Instruments, Switzerland, ultranano indentation tester) at an  
144 angle of  $141.9^\circ$ . In the first step, the indenter is placed on the sample surface  
145 by a rough approach at a speed of  $2000\text{ nm/min}$  until a contact force (set  
146 to  $15\ \mu\text{N}$ ) is detected. Then, force-displacement curves are acquired under  
147 imposed linear load/unload conditions. For gluten and starch, the maximum  
148 load was set to  $50\ \mu\text{N}$ , the loading/unloading rate to  $25\ \mu\text{N/min}$  and the  
149 pause time between loading and unloading to  $20\text{ s}$ . These parameter values  
150 were chosen to be as small as possible in order to avoid the sliding of the  
151 indenter. For bulk PMMA, these parameters were respectively set to  $100\ \mu\text{N}$ ,  
152  $50\ \mu\text{N/min}$  and  $30\text{ s}$  for most accurate measurements. The hardness  $H$  is  
153 defined as the ratio between the maximum force  $F_{max}$  just before unloading  
154 and the projected contact area  $A_N$  determined by the tip geometry. The  
155 indentation assays ( $n = 20$ ) were performed by displacements of  $10\ \mu\text{m}$ .

## 156 3. Results and Discussion

### 157 3.1. Evolution of abrasion depths

158 The AFM abrasion tests were performed on tablets prepared by powder  
159 compression to avoid slipping of the starch granule or the protein polymer  
160 along abrasion and also to avoid resin inclusion which may interact with  
161 the analyzed material and influence their mechanical properties. Due to  
162 potential variability of the polymers, reflecting their wheat origin or isolation  
163 method, the tablets were made of either commercially purchased purified  
164 starch and gluten or were extracted in the laboratory from wheat grains of  
165 different genetic background. The abrasion experiments were performed by  
166 a methodology derived from that of Ahimou et al. [27]. The AFM tip was

167 placed on a homogeneous gluten area or inside a starch granule, as shown in  
168 Figure 3 (a-b, a'-b'), and a square of  $1 \mu\text{m}^2$  area was scraped. The abrasion  
169 area was analyzed by means of  $5 \times 5 \mu\text{m}^2$  topographic images taken before  
170 and after  $N$  abrasion scans. As shown in Figure 3 (c and c'), the abrasion  
171 depth in gluten is higher than in starch for a similar applied normal force  
172 ( $F_N = 480 \text{ nN}$ ), which indicates a higher resistance to abrasion of starch  
173 compared to gluten.

174 Two different methods were used to measure the volume of the removed  
175 material. In fact, the potential lateral drift between successive acquired im-  
176 ages and the roughness of the scanned area makes it difficult to determine  
177 the total depth of the abraded area after ten abrasive scans. We used the  
178 differences between topographic images to measure the depth along the abra-  
179 sion path. The depth was obtained by averaging only in the central part of  
180 the path as the removed material is pushed to the edges. Therefore, the  
181 depth reached after  $N$  abrasion scans was calculated either as the difference  
182 between each topographic image and the initial image (before abrasion) or  
183 by cumulating the differences between successive images.

184 The results of the two methods for depth measurement are presented in  
185 Figure 4 for starch and gluten as well as an example of image subtraction.  
186 Values obtained by both methods almost coincide. However, the error in the  
187 first method (subtraction of each topographic image from the initial image)  
188 remains around 10% for the total depth after ten abrasive scans, which is  
189 below the 30% error in the second method. A linear increase of the depth  
190 was observed at the rates of  $11.3 \pm 4 \text{ nm}$  and  $1.57 \pm 0.9 \text{ nm}$  per abrasive  
191 scan for gluten and starch, respectively. Increasing the applied normal force  
192 from  $F_N = 480 \text{ nN}$  to  $F_N = 2600 \text{ nN}$  led to an increase of the depth after  
193 ten abrasive scans to  $111 \pm 28 \text{ nm}$  and  $15 \pm 4 \text{ nm}$  for gluten and starch,  
194 respectively.

195 The above depth data show clearly that gluten and starch have very dif-  
196 ferent mechanical properties irrespective of their genetic origin. This obser-  
197 vation is in strong contrast with earlier studies [14, 15]. It is also important  
198 to note that, as the abrasion depth and removed volumes are independent of  
199 the scan number, the mechanical behavior in the samples may be considered  
200 to be homogeneous.

### 201 3.2. Hardness starch and gluten determination

202 Due to the employed methodology, the abrasion process by the AFM tip  
203 can be interpreted as a linear scratching test usually performed to test the

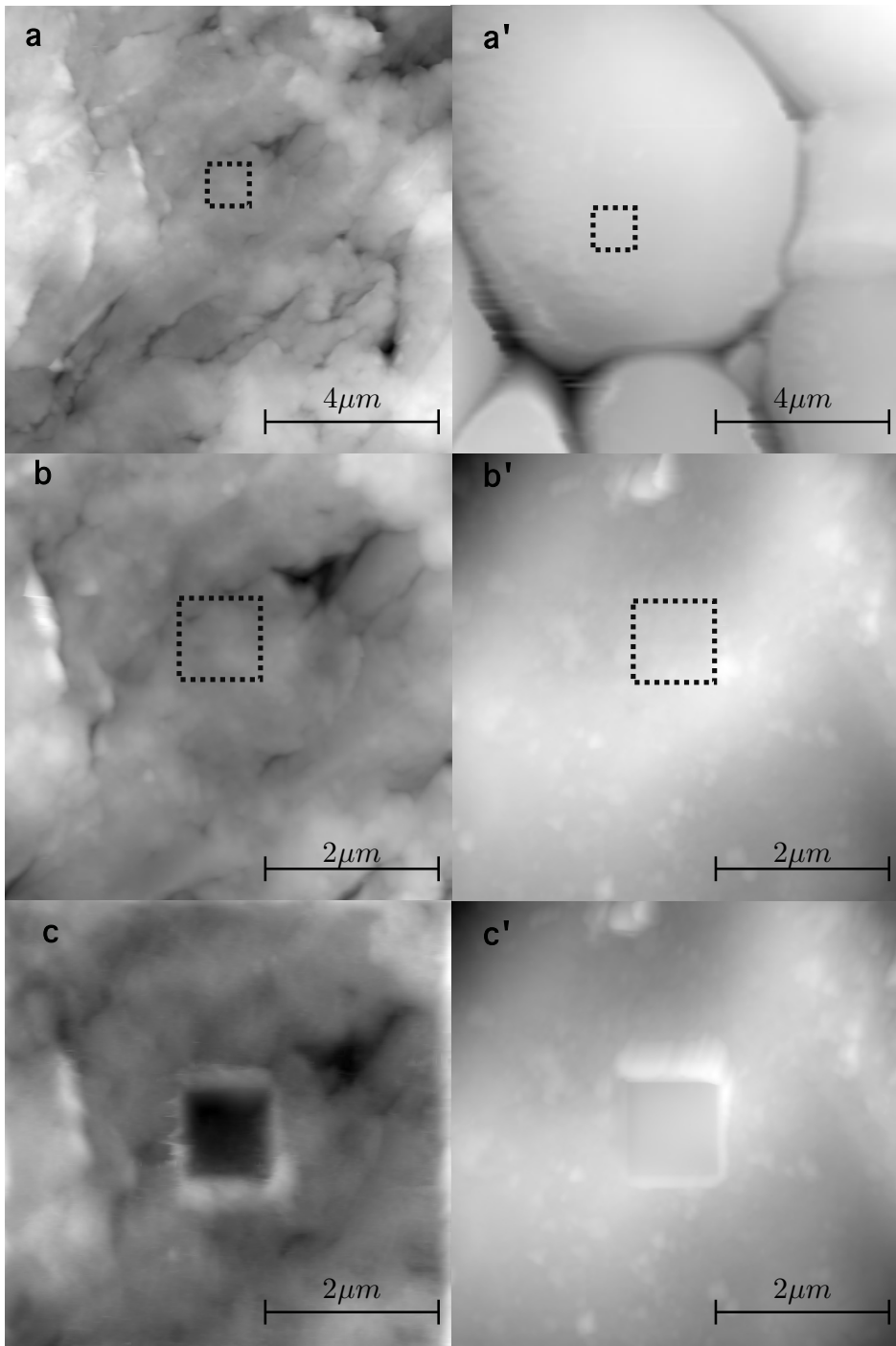


Figure 3: Examples of gluten (a-c) and starch (a'-c') AFM topographic images taken before abrasion at  $10 \times 10 \mu\text{m}^2$  (a, a') and  $5 \times 5 \mu\text{m}^2$  (b, b') and after 10 abrasive scans (c, c') with an applied normal force of 480 nN. The abrasion zone is marked into the figure with a square

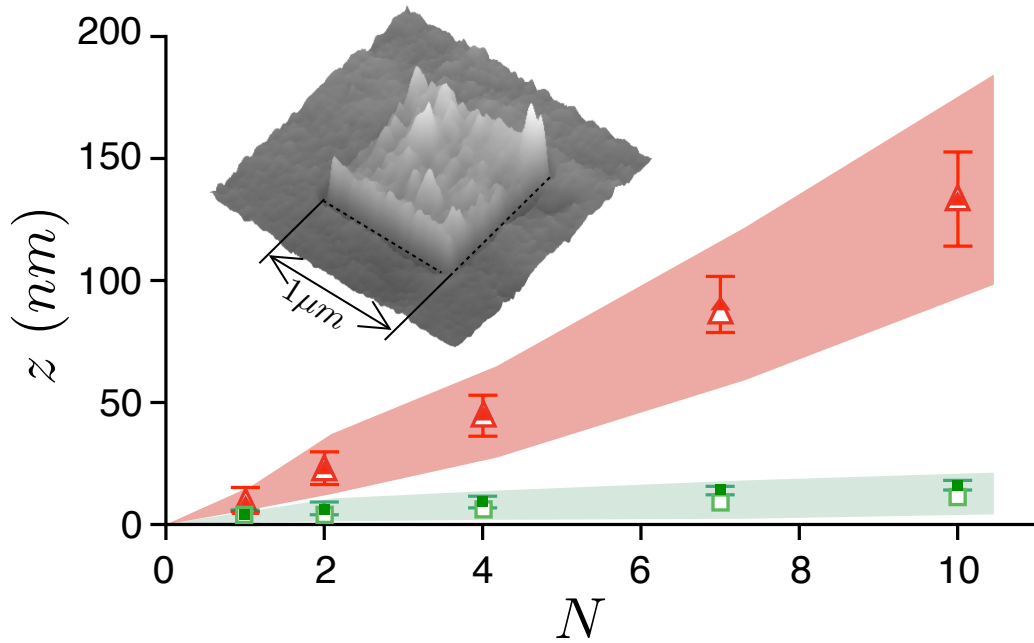


Figure 4: Illustration of different methods of depth ( $z$ ) measurement as a function of the abrasive scan number ( $N$ ) in gluten (red triangles) and starch (green squares) subjected to a normal force  $F_N = 480$  nN. For each biopolymer, the filled symbols and error bars correspond to the total difference between the scratched area and the initial topographic image whereas the empty symbols correspond to the cumulate of differences between successive images. The colored area corresponds to the maximum error obtained with this last method. The insert shows an example of a 3D image after subtraction between two images.

204 resistance of materials. Considering the trace and retrace tip displacement  
 205 over the abraded  $1 \mu\text{m}^2$  square area, the volume  $V$  of removed polymer after  
 206  $N$  iterated abrasive scans may be expressed as

$$V = 2n_\ell N L A_T \quad (1)$$

207 where  $n_\ell$  is the number of scan lines in the acquired topographic image (256  
 208 scanning lines),  $N$  is the number of scans,  $L$  is the length of the abraded  
 209 area ( $1 \mu\text{m}$ ) and  $A_T$  is the projected frontal area in contact with the tip as  
 210 schematized in Figure 2b. The validity of the above expression was checked  
 211 on PMMA by measuring the removed volume as a function of  $n_\ell$ , which was  
 212 changed from 128 to 1024 scanning lines (data not shown). As expected for a  
 213 linear scratching test, an increase of the removed volume was observed with  
 214 the number of scanning lines. Therefore, the cohesive energy determined by  
 215 [27] from the measured volume does not reflect only the intrinsic properties of  
 216 the analysed material although the data may still be sufficient to determine  
 217 mechanical properties such as the hardness.

218 The measurement of hardness requires the geometry of the indenter. The  
 219 apex radius of the AFM tip was given by the manufacturer to be below 10  
 220 nm but the tip wears off with calibration and reached a steady radius  $R$  value  
 221 (see experimental section) that remains stable during probing process. With  
 222 this spherical tip apex, the projected contact area  $A_N$  can be related to the  
 223 frontal area  $A_T$  by the following relation:

$$A_N = \pi(2RA_T)^{2/3} \quad (2)$$

224 By definition, the hardness  $H$  of a material is the ratio between the  
 225 applied normal force  $F_N$  and the area  $A_N$  under the tip (Figure 3b). Hence,  
 226 we get the following relation between  $H$  and  $F_N$ :

$$F_N = H\pi(2RA_T)^{2/3} \quad (3)$$

227 The data points for  $A_T$  for different values of  $F_N$  are plotted for starch and  
 228 gluten, as well as for PMMA, in Figure 5. The data are correctly fitted by  
 229 Eq. (3) allowing for the determination of hardness  $H$  for each polymer (Table  
 230 1).

231 The measured hardness of PMMA is consistent with previous data ob-  
 232 tained with distinct approaches yielding a value between 0.3 GPa and 0.6  
 233 GPa [31, 25, 32]. The hardness of gluten is found to be of the same order of

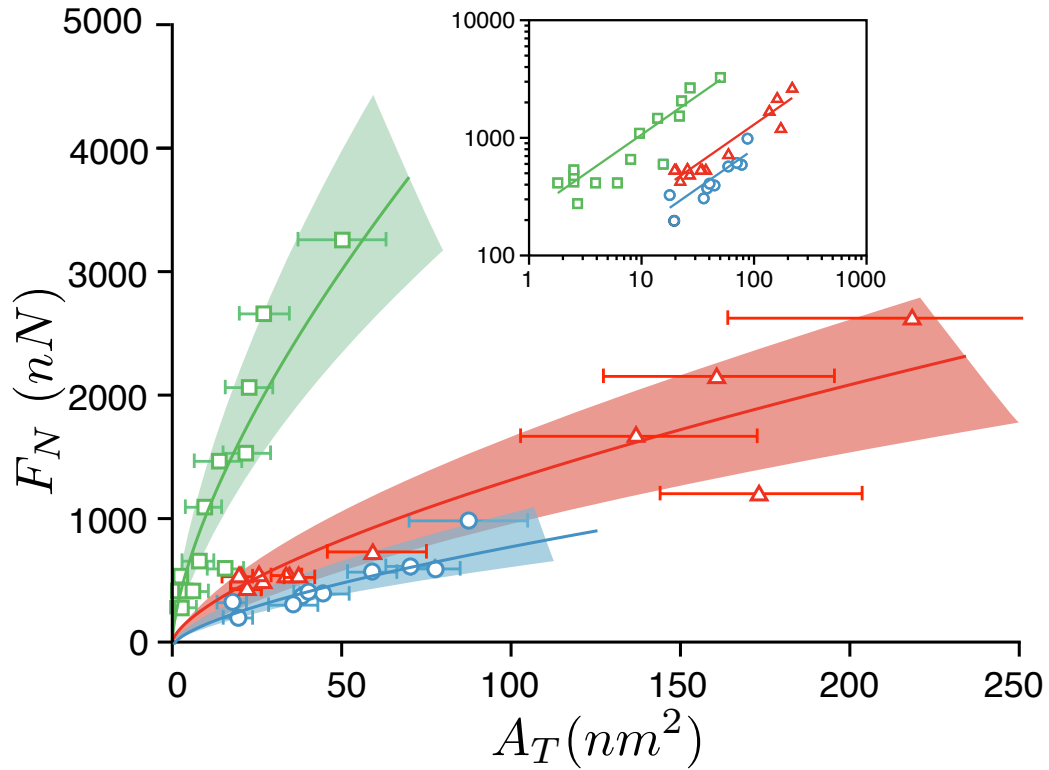


Figure 5: AFM data of the projected area  $A_T$  in front of the tip as a function of the normal force  $F_N$  for starch (green squares), gluten (red triangles) and PMMA (blue circles). Error bars on  $A_T$  represent measurement errors on the depth  $z$  and thus on the removed polymer volume  $V$  during abrasion. The full lines represent the predicted behavior by equation (3). The colored area around the fitting curve represents the error resulting from the tip radii variability. Insert: log-log representation of the same data.



234 magnitude as PMMA but four times lower than that of starch. The hardness  
 235 of gluten at the nanoscale is thus close to that of soft materials, such as  
 236 talc [35], and similar to other biopolymers such as wheat straw or other crop  
 237 stalks [36], whereas the starch hardness is closer to that of calcite [35] and  
 238 the values measured for core shells [37].

239 The observed hardness for starch and gluten is in a better agreement  
 240 with the differences in the structure of the two biopolymers than earlier  
 241 evaluations by micro-indentation [14, 15]. In fact, the gluten is characterized  
 242 by a complex protein network [39] whereas the starch has a granular and  
 243 semi-cristalline structure [43]. This discrepancy between our results at the  
 244 nano-scale and those of earlier measurements by micro-indentation may be  
 245 due to the scale of measurement or the orders of magnitude of the applied  
 246 forces, as already pointed out in the literature [35, 24, 37]. In fact, a close look  
 247 at the previous results obtained for wheat grains [15] or for purified starch  
 248 and gluten dispersed in a polyester resin [14] indicate that the indentation  
 249 depth was generally above 10  $\mu\text{m}$  for applied forces of several mN. Therefore,  
 250 at this resolution, the polymers in wheat grains are difficult to distinguish,  
 251 and hence the measurement reflects in practice the hardness of the softer  
 252 polymer. Furthermore, in Barlow et al. [14], the purified isolated polymers  
 253 were included in a resin which was prone to modify the polymer properties.  
 254 Indeed, the measured hardness of a single component in a composite material  
 255 was found to be highly dependent on the dimensions of indenter [38].

Table 1: Hardness  $H$  and apparent friction coefficient  $\mu_{app}$  obtained by AFM for gluten, starch and PMMA.

	$H$ (MPa)	$\mu_{app}$
Gluten	$640 \pm 170$	$0.39 \pm 0.05$
Starch	$2400 \pm 600$	$0.32 \pm 0.05$
PMMA	$400 \pm 100$	$0.59 \pm 0.05$

256 The mechanical properties of PMMA, as a bulk material, as obtained  
 257 with AFM were also compared with the data obtained by indentation at the  
 258 nanoscale. The nanoindentation assays confirmed the PMMA hardness even  
 259 with a better accuracy at  $420 \pm 30$  MPa, which is similar to those reported in  
 260 previous studies [31, 32]. But gluten and starch, which respectively display a  
 261 complex protein network and a granular structure [39, 3] were more difficult  
 262 to explore. A number of indentation tests on these two polymers had to be  
 263 discarded due to the sliding of the indenter during the assay. However, the

264 data obtained confirmed the difference between the two biopolymers with a  
 265 hardness between 400 and 760 MPa for gluten and between 1000 and 2600  
 266 MPa for starch. Nevertheless, we observed a higher variability of the mea-  
 267 surements for this type of polymers in nanoindentation assays.

### 268 3.3. Shear strength determination

269 The friction coefficient  $\mu_{app}$  at the interface between two solid bodies at  
 270 the nanoscale can be evaluated from the friction force  $F_T$ , recorded during  
 271 AFM nano-scratching test, and the applied normal force  $F_N$  [40, 25]:

$$\mu_{app} = \frac{F_T}{F_N} \quad (4)$$

272 Figure 6 shows the mean value of  $F_T$  versus  $F_N$  for each polymer. The data  
 273 collapse on a straight line passing through the origin. The apparent friction  
 274 coefficient  $\mu_{app}$  is given by the slope and its values are presented in Table 1.  
 275 The measured values of  $\mu_{app}$  are quite close for starch and gluten and about  
 276 1.5 to 2 times below that of PMMA<sup>2</sup>.

277 It is worth noting that this apparent friction coefficient  $\mu_{app}$  measured at  
 278 the nanoscale can not be directly interpreted as Amonton’s friction coefficient  
 279 measured at the macroscopic scale, where multi-asperity contact is assumed  
 280 [29]. In fact, in scratching of a soft material at the nanoscale, the apparent  
 281 friction occurs at a single asperity from the addition of two effects:

- 282 • Interfacial shear in a small layer of the material;
- 283 • Visco-elastoplastic flow of material around the scratching tip.

284 In all models described in the literature, the interfacial shear was character-  
 285 ized by adhesion or a real friction coefficient  $\mu_{true}$ , which is of special interest  
 286 as it is linked to the mechanical hardness through equation:

$$\mu_{true} = \frac{\tau}{H} \quad (5)$$

---

<sup>2</sup>The vanishing of the friction force with normal force means that  $F_N$  is the real contact reaction force including both the compressive force exerted vertically on the tip and the cohesive van der Waals force exerted by the surface on the AFM tip. This is because the reference state for the deflection of the cantilever is the force-free state, so that the deflection of the cantilever is the resultant of both the attraction force and compressive forces acting at the tip.

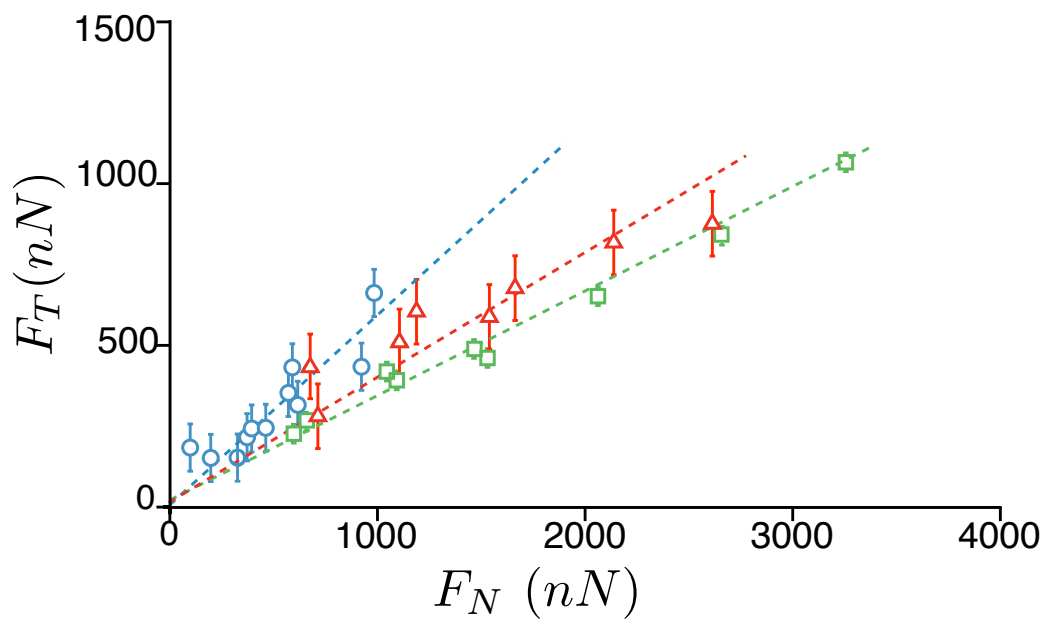


Figure 6: Friction force  $F_T$  plotted against normal force  $F_N$  for starch (green squares), gluten (red triangles) and PMMA (blue circles). The error bars represent the standard deviation of  $F_T$  for ten independent abrasive scans. The data are fitted by a straight line crossing the origin.

287 where  $\tau$  is the shear strength of the material. The measured apparent co-  
 288 efficient is thus comprised between the real friction coefficient and a higher  
 289 value [41], which depends on the behavior of the scratched material under  
 290 experimental conditions (applied forces, tip geometry, strain velocity, tem-  
 291 perature).

292 If the polymers were totally elastic, we would have  $\mu_{app} = \mu_{true}$  and the  
 293 shear strength could be estimated by equation (5). In this case, the values  
 294 of the shear strength  $\tau$  for gluten, starch and PMMA would be equal to  
 295 250 MPa, 768 MPa and 236 MPa, respectively. However, during the test,  
 296 the polymers are not in the elastic domain because of scratching and plastic  
 297 deformation leaving a track as observed in Figure 3, c-c'. Therefore, the  
 298 apparent friction coefficient  $\mu_{app}$  should be modified by subtracting the effect  
 299 of the front created ahead of the moving tip with a ploughing coefficient  
 300  $\mu_{plough}$ :

$$\mu_{true} = \mu_{app} - \mu_{plough} \quad (6)$$

301 The coefficient  $\mu_{plough}$  may be evaluated from the rear contact angle  $\omega$  in front  
 302 of the tip along the scratching assay and the radius of contact determined  
 303 by in-situ measurement on a homogeneous and transparent material [29].  
 304 However, in our AFM conditions, the measurement of those parameters were  
 305 not possible. But for PMMA it has a value between 0.1 and 0.2 according  
 306 to previously reported data [41, 42]. Taking into account the ploughing  
 307 correction,  $\mu_{true}$  is found to be comprised between 0.39 and  $0.49 \pm 0.05$ , and  
 308 thus the shear strength  $\tau$  is found to be between  $156 \pm 59$  MPa and  $196 \pm 68$   
 309 MPa. These values of  $\mu_{true}$  and  $\tau$  are consistent with the previous scratching  
 310 studies developed on PMMA using similar conditions of temperature, strain  
 311 rate and contact pressure but different method of mesurement [29].

312 Assuming that gluten and starch have a similar elasto-plastic behavior,  
 313 we may use the same value of  $\mu_{plough}$  in equation (6) to estimate  $\mu_{true}$  for  
 314 starch and gluten. The resulting shear strength is then comprised between  
 315  $122 \pm 64$  MPa and  $185 \pm 80$  MPa for gluten, thus close to that of PMMA,  
 316 and between  $288 \pm 192$  MPa and  $528 \pm 248$  MPa for starch. In all cases,  
 317 starch shows two to three times more strength than gluten in scratching  
 318 tests, supporting once more the difference in mechanical behavior of these  
 319 two biopolymers as it was already discussed with hardness measurements.

## 320 4. Conclusions

321 In this paper, AFM scratching assays were performed with two important  
322 biopolymers, starch and gluten. Our findings reveal a higher resistance to  
323 fracture and a less friction coefficient for starch compared to gluten, the later  
324 being closer to our reference material PMMA. These data will serve to refine  
325 a numerical model of the starchy endosperm fractionation process. Given  
326 the broad use of these two biopolymers in food and non-food products, the  
327 described method also appears helpful in order to further explore the me-  
328 chanical properties of starch and gluten in a wide range of conditions of tem-  
329 perature, relative humidity and stresses. In contrast with nanoindentation,  
330 this AFM scratching assay also allows to map the local mechanical properties  
331 and assess the potential heterogeneity of the material at a nanoscale level.  
332 This method thus appears an interesting alternative to characterize any type  
333 of polymers. It also opens the way to determine the mechanical properties  
334 of each of the components in a composite material and possibly the polymer  
335 interface.

## 336 5. Acknowledgement

337 We would like to thank F. Baudoin (UMR IATE, Montpellier) for his kind  
338 gift of wheat grain purified starch and gluten and S. Calas-Etienne (Univer-  
339 sity Montpellier 2) for the nano-indentation assays. We are also grateful to  
340 Montpellier 2 University and CEPIA department of INRA for the PhD grant  
341 of E. Chichti.

- 342 [1] F. Xie, P. J. Halley, L. Averous, Rheology to understand and optimize  
343 processibility, structures and properties of starch polymeric materials,  
344 *Prog. Polym. Sci.* 37 (4) (2012) 595–623.
- 345 [2] D. Zaidel, N. Chin, Y. Yusof, A review on rheological properties and  
346 measurements of dough and gluten, *J. Applied Sci.* 10 (20) (2010) 2478–  
347 2490.
- 348 [3] H. Cornell, The functionality of wheat starch. In *Starch in Food, Struc-  
349 ture Function and Applications*, Woodhead publishing Ld., Cambridge,  
350 UK, 2004, pp. 211–240.
- 351 [4] T. Evers, S. Millar, Cereal grain structure and development: Some im-  
352 plications for quality, *J. Cereal. Sci.* 36 (3) (2002) 261–284.

- 353 [5] L. Averous, Biodegradable multiphase systems based on plasticized  
354 starch: A review, *J. Macromol. Sci.-Pol. R. C44* (3) (2004) 231–274.  
355 doi:10.1081/mc-200029326.
- 356 [6] H. Zhang, G. Mittal, Biodegradable protein-based films from plant re-  
357 sources: A review, *Environmental Progress and Sustainable Energy*  
358 29 (2) (2010) 203–220. doi:10.1002/ep.10463.
- 359 [7] S. Guilbert, C. Guillaume, N. Gontard, *Food Engineering Series*,  
360 Springer, 2011, pp. 619–630.
- 361 [8] C. Andersson, New ways to enhance the functionality of paperboard  
362 by surface treatment - a review, *Packag. Technol. Sci.* 21 (6) (2008)  
363 339–373. doi:10.1002/pts.823.
- 364 [9] J. Jane, C. Maningat, R. Wongsagonsup, Starch characterization, vari-  
365 ety and application. In *Industrial crops and uses*, Singh, B. P., 2010, pp.  
366 207–235.
- 367 [10] Z. Wang, Z. Li, Z. Gu, Y. Hong, L. Cheng, Preparation, characterization  
368 and properties of starch-based wood adhesive, *Carbohydr. Polym.* 88 (2)  
369 (2012) 699–706. doi:10.1016/j.carbpol.2012.01.023.
- 370 [11] S. Khosravi, P. Nordqvist, F. Khabbaz, M. Johansson, Protein-based ad-  
371 hesives for particleboards-effect of application process, *Ind. Crop. Prod.*  
372 34 (3) (2011) 1509–1515. doi:10.1016/j.indcrop.2011.05.009.
- 373 [12] V. Topin, J.-Y. Delenne, F. Radjai, L. Brendel, F. Mabilie, Strength and  
374 failure of cemented granular matter, *Eur Phys J E Soft Matter* 23 (4)  
375 (2007) 413–29. doi:10.1140/epje/i2007-10201-9.
- 376 [13] V. Topin, F. Radjai, J.-Y. Delenne, F. Mabilie, Mechanical modeling of  
377 wheat hardness and fragmentation, *Powder Technol.* 190 (1-2) (2009)  
378 215–220. doi:10.1016/j.powtec.2008.04.070.
- 379 [14] K. K. Barlow, M. S. Buttrose, D. H. Simmonds, M. Vesik, The nature  
380 of the starch-protein interface in wheat endosperm, *Cereal Chem.* 50  
381 (1973) 443–454.
- 382 [15] G. M. Glenn, R. K. Johnston, Mechanical-properties of starch, protein  
383 and endosperm and their relationship to hardness in wheat, *Food Struct.*  
384 11 (3) (1992) 187–199.

- 385 [16] G. Binnig, C. F. Quate, C. Gerber, Atomic force microscope, *Phys. Rev.*  
386 *Lett.* 56 (9) (1986) 930–933. doi:10.1103/PhysRevLett.56.930.
- 387 [17] D. Fotiadis, S. Scheuring, S. A. Muller, A. Engel, D. J. Muller, Imaging  
388 and manipulation of biological structures with the afm, *Micron* 33 (4)  
389 (2002) 385–397. doi:10.1016/S0968-4328(01)00026-9.
- 390 [18] N. C. Santos, M. A. R. B. Castanho, An overview of the biophysical  
391 applications of atomic force microscopy, *Biophys. Chem.* 107 (2) (2004)  
392 133–149. doi:10.1016/j.bpc.2003.09.001.
- 393 [19] P. M. Baldwin, J. Adler, M. C. Davies, C. D. Melia, High resolution  
394 imaging of starch granule surfaces by atomic force microscopy, *J. Cereal.*  
395 *Sci.* 27 (3) (1998) 255–265. doi:10.1006/jcrs.1998.0189.
- 396 [20] S. Neethirajan, D. J. Thomson, D. S. Jayas, N. D. G. White, Character-  
397 ization of the surface morphology of durum wheat starch granules using  
398 atomic force microscopy, *Microsc. Res. Techniq.* 71 (2) (2008) 125–132.  
399 doi:10.1002/jemt.20534.
- 400 [21] A. Paananen, K. Tappura, A. S. Tatham, R. Fido, P. R. Shewry,  
401 M. Miles, T. J. McMaster, Nanomechanical force measurements  
402 of gliadin protein interactions, *Biopolymers* 83 (6) (2006) 658–667.  
403 doi:10.1002/bip.20603.
- 404 [22] A. D. L. Humphris, T. J. McMaster, M. J. Miles, S. M. Gilbert, P. R.  
405 Shewry, A. S. Tatham, Atomic force microscopy (afm) study of inter-  
406 actions of hmw subunits of wheat glutenin, *Cereal Chem.* 77 (2) (2000)  
407 107–110. doi:10.1094/CCHEM.2000.77.2.107.
- 408 [23] L. Scudiero, C. F. Morris, Field emission scanning electron and  
409 atomic force microscopy, and raman and x-ray photoelectron spec-  
410 troscopy characterization of near-isogenic soft and hard wheat ker-  
411 nels and corresponding flours, *J. Cereal Sci.* 52 (2) (2010) 136–142.  
412 doi:10.1016/j.jcs.2010.04.005.
- 413 [24] B. Bhushan, X. D. Li, Nanomechanical characterisation of solid  
414 surfaces and thin films, *Int. Mater. Rev.* 48 (3) (2003) 125–164.  
415 doi:10.1179/095066003225010227.

- 416 [25] S. E. Flores, M. G. Pontin, F. W. Zok, Scratching of elastic/plastic  
417 materials with hard spherical indenters, *J. Appl. Mech.-T. ASME* 75 (6)  
418 (2008) 061021. doi:10.1115/1.2966268.
- 419 [26] N. E. Kurland, Z. Drira, V. K. Yadavalli, Measurement of nanomechanical  
420 properties of biomolecules using atomic force microscopy, *Micron*  
421 43 (2-3) (2012) 116–128. doi:10.1016/j.micron.2011.07.017.
- 422 [27] F. Ahimou, M. J. Semmens, P. Novak, G. Haugstad, Biofilm cohesive  
423 measurement using a novel atomic force microscopy methodology, *Ap-  
424 plied Environ. Microbiol.* 73 (9) (2007) 2897–2904.
- 425 [28] S. Lafaye, M. Troyon, On the friction behaviour in nanoscratch testing,  
426 *Wear* 261 (7-8) (2006) 905–913. doi:10.1016/j.wear.2006.01.036.
- 427 [29] S. Lafaye, C. Gauthier, R. Schirrer, Analysis of the apparent fric-  
428 tion of polymeric surfaces, *J. Mater. Sci.* 41 (19) (2006) 6441–6452.  
429 doi:10.1007/s10853-006-0710-7.
- 430 [30] F. Auger, M.-H. Morel, M. Dewilde, A. Redl, Mixing history affects  
431 gluten protein recovery, purity, and glutenin re-assembly capacity from  
432 optimally developed flour-water batters, *J. Cereal Sci.* 49 (3) (2009)  
433 405–412. doi:10.1016/j.jcs.2009.01.008.
- 434 [31] A. Karimzadeh, M. R. Ayatollahi, Investigation of mechanical and  
435 tribological properties of bone cement by nano-indentation and  
436 nano-scratch experiments, *Polym. Test.* 31 (6) (2012) 828–833.  
437 doi:10.1016/j.polymertesting.2012.06.002.
- 438 [32] G. H. Wei, B. Bhushan, N. Ferrell, D. Hansford, Microfabrication  
439 and nanomechanical characterization of polymer microelectromechan-  
440 ical system for biological applications, *J. Vac. Sci. Technol. A* 23 (4)  
441 (2005) 811–819. doi:10.1116/1.1861937.
- 442 [33] J. L. Hutter, J. Bechhoefer, Calibration of atomic-force microscope tips  
443 (vol 64, pg 1868, 1993), *Rev. Sci. Instrum.* 64 (11) (1993) 3342–3342.  
444 doi:10.1063/1.1144449.
- 445 [34] B. D. Morton, H. Wang, R. A. Fleming, M. Zou, Nanoscale surface  
446 engineering with deformation-resistant core-shell nanostructures, *Tribol.  
447 Lett.* 42 (1) (2011) 51–58. doi:10.1007/s11249-011-9747-0.



- 448 [35] J. A. Williams, Analytical models of scratch harness, *Tribology Int.* 29  
449 (1996) 675–694.
- 450 [36] Y. Wu, S. Wang, D. Zhou, C. Xing, Y. Zhang, Z. Cai, Evaluation  
451 of elastic modulus and hardness of crop stalks cell walls by  
452 nano-indentation, *Bioresource Technol.* 101 (8) (2010) 2867–2871.  
453 doi:10.1016/j.biortech.2009.10.074.
- 454 [37] T. Shean, M. Oyen, M. Ashby, *Handbook of nanoindentation with bio-*  
455 *logical applications*, Pan Stanford Pub., Singapore, 2011, pp. 1–22.
- 456 [38] C. Scheuerlein, T. Boutboul, D. Leroy, L. Oberli, B. Rehmer, Hardness  
457 and tensile strength of multifilamentary metal-matrix composite super-  
458 conductors for the large hadron collider (lhc), *J. Mater. Sci.* 42 (12)  
459 (2007) 4298–4307. doi:10.1007/s10853-006-0633-3.
- 460 [39] V. Kontogiorgos, Microstructure of hydrated gluten network, *Food. Res.*  
461 *Int.* 44 (9) (2011) 2582–2586. doi:10.1016/j.foodres.2011.06.021.
- 462 [40] F. Bowden, D. Tabor, *The friction and lubrication of solids*, Oxford  
463 University Press, London, 1951.
- 464 [41] S. Lafaye, C. Gauthier, R. Schirrer, A surface flow line model of a  
465 scratching tip: apparent and true local friction coefficients, *Tribol. Int.*  
466 38 (2) (2005) 113–127. doi:10.1016/j.triboint.2004.06.006.
- 467 [42] S. Lafaye, C. Gauthier, R. Schirrer, The ploughing friction: analytical  
468 model with elastic recovery for a conical tip with a blunted spherical  
469 extremity, *Tribol. Lett.* 21 (2) (2006) 95–99. doi:10.1007/s11249-006-  
470 9018-7.
- 471 [43] A. Buleon, P. Colonna, V. Olanhot, Starch granules: structure and  
472 biosynthesis, *Int. J. Biol. Macromol.* 23 (1998) 85–112.